Forces between Two Colloidal Particles in a Nematic Solvent†

Muataz S. Al-Barwani

Department of Physics, College of Science, Sultan Qaboos University, P.O. Box 36, Al-Khod 123, Muscat, Sultanate of Oman

Gregory S. Sutcliffe and Michael P. Allen*

Centre for Scientific Computing and Department of Physics, University of Warwick, CV4 7AL, Coventry, United Kingdom

Received: November 30, 2003; In Final Form: January 29, 2004

We use molecular dynamics to study the structure around two spherical colloidal particles embedded in a nematic liquid crystal host. By studying nematic ordering in the region between the two particles we are able to examine the effects of the presence of multiple particles on a nematic. In addition, we study the forces on the particles as functions of the separation between the two colloidal particles and their orientation with respect to the nematic director.

1. Introduction

Dispersions of small particles in a host fluid are a widespread and important state of matter; colloidal suspensions are dispersions of solid particles, whereas emulsions are dispersions of liquid droplets coated with a surfactant. They are of considerable technological importance, with applications in everything from paints and coatings to foods and drugs.[1] These are metastable rather than equilibrium systems. Attractive interactions among the particles, which arise, for example, from dispersion forces or the depletion interaction, can separate the dispersed phase from the host fluid. These forces must be counterbalanced by Coulombic, steric, or other repulsive interactions. The delicate balance between attractive and repulsive colloidal interactions determines the stability and hence the usefulness of dispersions.

Colloidal suspensions in a liquid crystal matrix are qualitatively different from their isotropic analogues due to the long-range deformation of the director field **n**(**r**) created by particles in the liquid crystal.[2] The effect of a suspended particle on the orientational order in its surroundings will depend on the strength and type of director anchoring on its surface. Particles with weak anchoring will disturb the static director very little. Particles with strong anchoring on the other hand, would create a topological mismatch with the otherwise uniform director field and develop singularities or defects. Several simulation studies have been carried out to investigate such topological defects caused by spherical[3] and rodlike[4,5] particles with interesting results. Our interest in this paper lies in small spherical particles, for which the surrounding defect structure takes the form of a Saturn ring around the equator, or a point satellite defect at one of the poles, depending on the radius and anchoring strength.The geometry of the system is defined in Figure 1. We denote the vector between the particle centers **d**, of length d; the angle between the far-field director **n** and **d** is denoted θ.

Previous experimental studies have shown that the interaction between particles in a nematic phase is attractive at large distances and repulsive at short distances. The effects are seen in the dispersion of water droplets in the nematic liquid crystal pentylcyanobiphenyl (5CB).[1] The droplets form linear chains without approaching each other too closely. Theoretical studies based on a continuum elastic treatment of the nematic phase[2,6] have predicted that, within the one-elastic-constant approximation and to leading order in inverse powers of separation, the interaction potential between two spheres in a nematic phase is anisotropic and is of the form

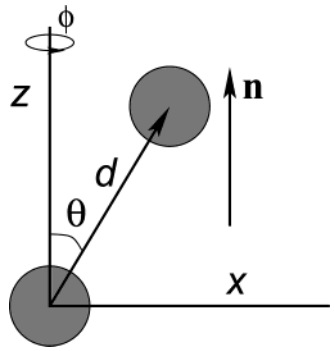

Figure 1. Geometry of the two-particle system. The far-field director is denoted **n**, and the center−center vector is **d**.

$$U \propto d^{-5}[9 - 20\cos 2\Psi + 35\cos 4\Psi] \qquad (1)$$

where $\Psi = \pi/2 - \theta$. The constant of proportionality depends on the Frank elastic constant, the surface anchoring strength, and the particle radius. A key point is that the angular dependence is independent of these physical parameters, and the potential has minima with respect to angular variation at $\Psi = (1/2)\arctan(4\sqrt{3}) \approx \pm 41°$, that is at $\theta \approx 49°, 131°$. This angular dependence also implies that the nature of the interaction − attractive or repulsive − changes depending on the orientation of the axis connecting the two particles relative to the nematic director n.

In this paper, we present the results of molecular dynamics (MD) simulations of two spherical particles immersed in a bulk nematic mesophase. Using MD we study the forces on the particles for different separations and orientations with respect to the nematic director.

† Part of the special issue "Hans C. Andersen Festschrift".

10.1021/jp037650k CCC: $27.50
Published on Web 03/16/2004

The paper is organized as follows. In Sec 2 we present the computational details and molecular models we use to simulate the liquid crystal mesophase and the interaction of the molecules with the particle surface. Section 3 contains the results of the simulations: density, director and order parameter maps for different separations and orientations. We also present the force calculations on each particle as functions of separation and orientation and compare our results to the theoretical predictions. Concluding remarks are given in Section 4.

2. Molecular Model and Simulation Methods

Molecular dynamics simulations were carried out using axially symmetric molecules interacting through the repulsive Gay−Berne pair potential

$$v_{ij}(\mathbf{r}_{ij},\mathbf{u}_i,\mathbf{u}_j) = \begin{cases} 4\epsilon_0(\rho_{ij}^{-12} - \rho_{ij}^{-6}) + \epsilon_0 & \rho_{ij}^{6} < 2 \\ 0 & \rho_{ij}^{6} > 2 \end{cases} \quad (2)$$

Here $\rho_{ij} = (r_{ij} - \sigma_{ij} + \sigma_0)/\sigma_0$; r_{ij} is the center-center separation, σ_0 a size parameter, ϵ_0 an energy parameter (both taken to be unity henceforth), and the orientation-dependent diameter σ_{ij} is defined by

$$\sigma_{ij} = \sigma_0\left\{1 - \frac{\chi}{2}\left[\frac{(\hat{\mathbf{r}}_{ij}\cdot\mathbf{u}_i + \hat{\mathbf{r}}_{ij}\cdot\mathbf{u}_j)^2}{1+\chi(\mathbf{u}_i\cdot\mathbf{u}_j)} + \frac{(\hat{\mathbf{r}}_{ij}\cdot\mathbf{u}_i - \hat{\mathbf{r}}_{ij}\cdot\mathbf{u}_j)^2}{1-\chi(\mathbf{u}_i\cdot\mathbf{u}_j)}\right]\right\}^{-1/2}$$

where $\chi = (\kappa^2 - 1)/(\kappa^2 + 1)$, κ being the elongation. The orientation dependence is written in terms of the direction of the center−center vector $\hat{\mathbf{r}}_{ij} = \mathbf{r}_{ij}/r_{ij}$ and the unit vectors $\mathbf{u}_i,\mathbf{u}_j$, which specify the molecular symmetry axes. This is a soft repulsive potential, approximately describing ellipsoidal molecules and is a variant of the standard Gay−Berne potential[7,8] with exponents $\mu = 0,\nu = 0$.

The interaction of molecule i with each of the colloidal particles was given by a shifted Lennard-Jones repulsion potential between the centers, having exactly the same form as eq 2, but with ρ_{ij} replaced by

$$\rho_{i\pm} = \frac{|\mathbf{r}_i - \mathbf{r}_\pm| - R + \sigma_0}{\sigma_0}$$

Here, R is the spherical particle radius, and $\mathbf{r}_\pm$ are the positions of the two sphere centers, with $\mathbf{r}_+ - \mathbf{r}_- = \mathbf{d}$. The interaction potential results in homeotropic anchoring of the liquid crystal molecules, normal to the colloidal particle surface.

The colloidal systems consisted of $N = 64\,000$ ellipsoidal molecules with elongation $\kappa = 3$, surrounding two spheres of radius $R/\sigma_0 = 3$ and separation d/σ_0 in the range $9 \le d/\sigma_0 \le 15$ (corresponding to a surface-surface distance $3 \le s/\sigma_0 \le 9$). A reduced temperature of $k_BT/\epsilon_0 = 1$ was used throughout (for this model, the phase behavior is not sensitively dependent on temperature, as there are no attractive forces). The system size was chosen so that the number density of the liquid crystal far from the spherical particles was $\rho\sigma_0^3 = 0.34$, which lies well within the nematic region. For this system, in reduced units defined by σ_0, ϵ_0, and m, a time step $\delta t = 0.004$ was found suitable. The molecular mass m was taken to be unity, and the molecular moment of inertia fixed as $I = 2.5m\sigma_0^2$.

Previous studies of single colloidal particles[3] have shown that, for this radius, the nematic solvent adopts a Saturn ring defect structure around the particle equator. The distortion of the director configuration, and the interaction between the defects as the spheres approach each other, are the principal objects of study here.

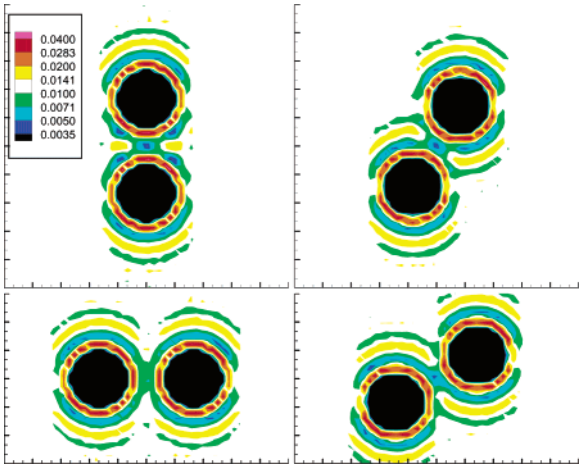

Figure 2. Local nematic number density $\rho(\mathbf{r})$ around the colloidal particles, in a slice in the $\mathbf{n}-\mathbf{d}$ plane. The separation is $d = 10\sigma_0$ with (clockwise from top left) angles $\theta = 0°$, 30°, 60°, and 90°. Color coding is chosen so that the average density in the bulk nematic is white.

Cubic periodic boundary conditions were employed in all the simulations. The simulations employed a domain decomposition program on a massively parallel cluster computer. A global constraint was applied to fix the orientation of the director along the z axis. The production run for every orientation and separation was 10^6 steps, with a prior equilibration run of a similar length.

The forces on each colloidal particle $\mathbf{F}_\pm$ were calculated using the total force $\mathbf{f}_{i\pm}$ on it from each molecule i in the solvent,

$$\mathbf{F}_\pm = -\sum_{i=1}^{N}\mathbf{f}_{i\pm}$$

These forces were averaged over the entire production runs, with the spheres held in fixed positions. Statistical errors in these results were estimated on the basis of a normal distribution of subaverages, taking care to check for the effect of serial correlations by studying the dependence on the sub-average lengths.

The local order tensor $\mathbf{Q}(\mathbf{r})$ was calculated on a regular grid in the simulation box, as follows:

$$Q_{\alpha\beta} = \frac{1}{n}\sum_{k=1}^{n}\frac{3}{2}\langle u_{k\alpha}u_{k\beta}\rangle - \frac{1}{2}\delta_{\alpha\beta}$$

where there are n molecules present in a defined volume around each grid point, $\delta_{\alpha\beta}$ is the Kronecker delta, $\langle ...\rangle$ denotes an ensemble average, $\alpha, \beta = x, y, z$. Diagonalizing the $Q_{\alpha\beta}$ tensor, for each grid point, gives the three eigenvalues, plus the three corresponding eigenvectors. The largest eigenvalue defines the order parameter $S(\mathbf{r})$ at each point, and the corresponding eigenvector is the local director $\mathbf{n}(\mathbf{r})$.

3. Results

Simulations were performed for angles $0° \le \theta \le 90°$ at intervals of 15°, and for a range of colloidal particle separations $9\sigma_0 \le d \le 12\sigma_0$ in steps of $0.5\sigma_0$, and additionally $d = 15\sigma_0$. The local nematic density around the particles, for a separation $d = 10\sigma_0$ and various angles θ, is shown in Figure 2. The regions of low density near the particle equators are visible. At this separation, there is a depletion region between the spheres. The corresponding maps of nematic order parameter are shown in Figure 3. In this figure the Saturn ring defects are clearly visible.

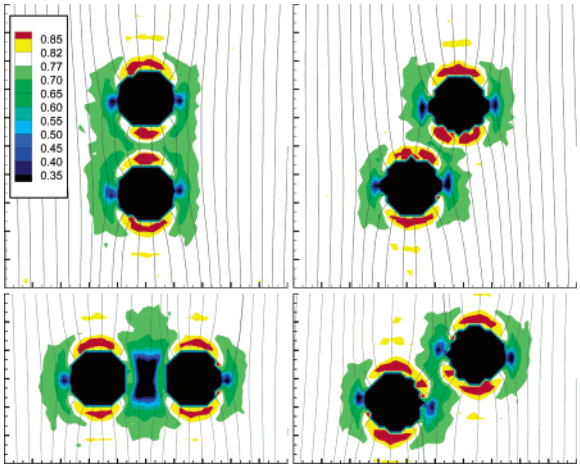

Figure 3. Local nematic order parameter $S(\mathbf{r})$ around the colloidal particles, in a slice in the $\mathbf{n}-\mathbf{d}$ plane. The separation is $d = 10\sigma_0$ with (clockwise from top left) angles $\theta = 0°$, 30°, 60°, and 90°. Color coding is chosen so that the average order in the bulk nematic is white. Superimposed on the map are streamlines of the local director field $\mathbf{n}(\mathbf{r})$.

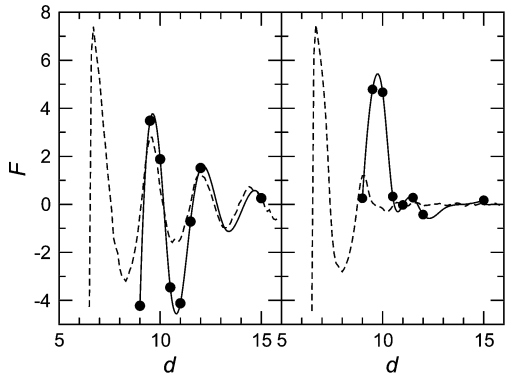

Figure 4. Component of the solvent-mediated interparticle force parallel to the line of centers for $\theta = 0°$ (left) and $\theta = 90°$ (right). The symbols denote simulation averages; error bars are smaller than the plotting symbol in all cases. The solid lines are to guide the eye. The dashed lines represent $(-\partial/\partial r)k_BT \ln \rho(\mathbf{r})$, where $\rho(\mathbf{r})$ is the fluid density around an isolated sphere, horizontally shifted as discussed in the text.

It is convenient to resolve the force between the colloidal particles into components parallel, and perpendicular, to the center-center vector **d**. The parallel component is strongly dominated by effects reflecting the local structure at the molecular level: solvation and depletion. In Figure 4 we show two examples of the dependence of this force on separation d, for the cases $\theta = 0°$ and $\theta = 90°$. At $\theta = 0°$, and at all angles except those very close to $\theta = 90°$, the force varies in a highly oscillatory fashion with separation, as one would expect for highly ordered layers intervening between the colloidal particle surfaces. To predict this accurately would require a density-functional theory, which we do not present here. However, for comparison purposes only, we plot in Figure 4 the "mean force"

$$-\frac{\partial}{\partial r}k_BT \ln \rho(\mathbf{r})$$

felt by a liquid crystal molecule in the vicinity of an isolated colloidal sphere. Here $\rho(\mathbf{r})$ is the local density measured near a single sphere in the corresponding θ direction; k_B is Boltzmann's constant. The resultant curve is shifted by $2R$ to account for the size of the particles. As can be seen, the approximate order of magnitude and oscillatory form of the interparticle force reflect the behavior of this curve.

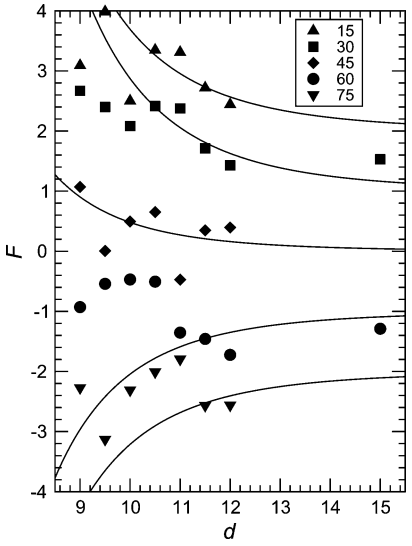

Figure 5. Component of the solvent-mediated interparticle force perpendicular to the line of centers for $\theta = 15-75°$. The symbols denote simulation averages; error bars are smaller than the plotting symbol in all cases. The solid lines are a one-parameter fit to eq 1. Successive sets of results are displaced vertically by one unit for clarity.

For the case $\theta = 90°$, the dependence of the parallel component of the force, on particle separation, is significantly different. The large oscillations are quickly damped out, due to the coalescence of the "melted" regions of nematic phase associated with the defects directly between the spheres. This behavior qualitatively echoes the form of the single-molecule "mean force" curve deduced from the density, although the quantitative comparison is not accurate. It is to be re-emphasized that this comparison has no rigorous foundation, it is merely to illustrate the general origins of the force, parallel to the line of centers, as distinct from the elastic forces considered in the theory leading to eq 1.

The perpendicular component of the force shows different behavior. For an isotropic solvent medium, this component would be rigorously zero. We observe that some structural variation is superimposed on a systematic trend that compares surprisingly well with the elastic theory prediction of eq 1. To illustrate this, we compare, in Figure 5, with a one-parameter fit (the overall strength parameter) to eq 1, all the perpendicular force data. The key feature of that equation, that the tendency of the perpendicular force is to favor alignment of the colloidal particles at $\theta \approx 49°$, is borne out reasonably well by our simulation results. Of course, one should not be surprised to see significant deviations from the elastic theory at such close separations, and the variation with d has much more structure.

4. Conclusions

Molecular dynamics techniques were used to study a system consisting of two spherical colloidal particles immersed in a nematic liquid crystal solvent consisting of 64 000 ellipsoidal molecules. The solvent structure and solvent-mediated interparticle interaction were studied as a function of both the magnitude and direction of the separation vector.

The force on each colloidal particle for each separation and orientation was calculated and a comparison was made with theoretical predictions. Additionally, density and order parameter maps were studied to further understand the nature of the forces which were mainly found to be depletion and solvation forces. The component of the force parallel to the intermolecular vector is strongly influenced by molecular-scale packing effects, and

for most angles of approach it tends to be highly oscillatory, reflecting the local fluid density between the colloidal particles. When the particles approach each other along a direction normal to the director, these oscillations are damped out, for distances comparable with, and larger than, the coalescence distance for the Saturn ring defects. The component perpendicular to the intermolecular vector is also influenced by molecular scale effects, but it is possible to detect some influence of liquid crystalline elastic behavior. The main prediction of the elastic theory, that the perpendicular forces favor alignment at a specific angle, seems to hold even at relatively small distances. It is instructive to compare this work with the analogous study of infinite rodlike particles,[5] for which the theoretical analysis has been taken somewhat further than here.

Finally, it should be noted that, in experimental work,[1] the sizes of the suspended particles are of the order $1-5\ \mu$m, much larger than the sizes (a few molecular diameters) studied here. Molecular simulations at such a scale, to make a direct comparison with experiment, would require a larger volume and an even larger number of liquid crystal molecules. This would make it computationally quite expensive, and a mesoscopic simulation method may be the only practical approach.

Acknowledgment. We thank Denis Andrienko for his help and useful discussions. Also, we thank members of the Complex Fluids Consortium, whose program GBMEGA was used in this work. This research was supported by Sultan Qaboos University internal grant IG/SCI/PHY/02/03 toward a research visit for M.S.A.B. to the Centre for Scientific Computing, University of Warwick. The computing facilities were provided by the Centre for Scientific Computing, with support from Joint Research Equipment Initiative grant JR00WASTEQ.

References and Notes

(1) Poulin, P.; Stark, H.; Lubensky, T. C.; Weitz, D. A. *Science* **1997**, *275*, 1770−1773.
(2) Ruhwandl, R. W.; Terentjev, E. M. *Phys. Rev. E* **1997**, *55*, 2958−2961.
(3) Andrienko, D.; Germano, G.; Allen, M. P. *Phys. Rev. E* **2001**, *63*, 041701/1−8.
(4) Andrienko, D.; Allen, M. P.; Skačej, G.; Žumer, S. *Phys. Rev. E* **2002**, *65*, 041702/1−7.
(5) Andrienko, D.; Tasinkevych, M.; Patricio, P.; Allen, M. P.; Telo da Gama, M. M. *Phys. Rev. E* **2003**, *68*.
(6) Ramaswamy, S.; Nityananda, R.; Raghunathan, V. A.; Prost, J. *Mol. Cryst. Liq. Cryst.* **1996**, *288*, 175−180.
(7) Berne, B. J.; Pechukas, P. *J. Chem. Phys.* **1972**, *56*, 4213−4216.
(8) Gay, J. G.; Berne, B. J. *J. Chem. Phys.* **1981**, *74*, 3316−3319.